

RESEARCH

Open Access



Co-culture of human AT2 cells with fibroblasts reveals a MUC5B phenotype: insights from an organoid model

Yiwen Yao^{1,2}, Felix Ritzmann¹, Sarah Miethe³, Kathrin Kattler-Lackes⁴, Betül Colakoglu¹, Christian Herr¹, Andreas Kamyschnikow¹, Michelle Brand¹, Holger Garn³, Daniela Yildiz⁶, Frank Langer⁷, Robert Bals^{1,5} and Christoph Beisswenger^{1*}

Abstract

Impaired interaction of fibroblasts with pneumocytes contributes to the progression of chronic lung disease such as idiopathic pulmonary fibrosis (IPF). Mucin 5B (MUC5B) is associated with IPF. Here we analyzed the interaction of primary fibroblasts and alveolar type 2 (AT2) pneumocytes in the organoid model. Single-cell analysis, histology, and qRT-PCR revealed that fibroblasts expressing high levels of fibrosis markers regulate STAT3 signaling in AT2 cells, which is accompanied by cystic organoid growth and MUC5B expression. Cystic growth and MUC5B expression were also caused by the cytokine IL-6. The PI3K-Akt signaling pathway was activated in fibroblasts. The drug dasatinib prevented the formation of MUC5B-expressing cystic organoids. MUC5B associated with AT2 cells in samples obtained from IPF patients. Our model shows that fibrotic primary fibroblasts induce impaired differentiation of AT2 cells via STAT3 signaling pathways, as observed in IPF patients. It can be used for mechanistic studies and drug development.

Keywords Organoid, Pneumocyte, Fibroblast, STAT3, IPF

*Correspondence:

Christoph Beisswenger
christoph.beisswenger@uks.eu

¹Department of Internal Medicine V – Pulmonology, Allergology and Critical Care Medicine, Saarland University, 66421 Homburg, Germany

²Department of Clinical Medicine, Shanghai Tongji Hospital, School of Medicine, Tongji University, 200065 Shanghai, China

³Translational Inflammation Research Division & Core Facility for Single Cell Multiomics, Medical Faculty, Member of the German Center for Lung Research (DZL) and the Universities of Giessen and Marburg Lung Center, Philipps University of Marburg, D-35043 Marburg, Germany

⁴Department of Genetics/Epigenetics, Saarland University, 66123 Saarbrücken, Germany

⁵Department of Drug Delivery (DDEL), Helmholtz-Institute for Pharmaceutical Research Saarland (HIPS), Helmholtz Centre for Infection Research (HZI), Saarbrücken, Germany

⁶Experimental and Clinical Pharmacology and Toxicology, PZMS, Saarland University, 66421 Homburg, Germany

⁷Department of Thoracic- and Cardiovascular Surgery, Saarland University Hospital, Homburg/Saar, Germany

Introduction

Gas exchange in the lung takes place in millions of alveoli. The alveolar epithelium consists of cuboidal alveolar type 2 (AT2) pneumocytes, which secrete various factors such as surface tension-lowering surfactants, and flat AT1 pneumocytes, which make up most of the alveolar surface for gas exchange (Milad and Morissette 2021). The proper interaction of the pneumocytes with numerous other cell types such as alveolar fibroblasts is essential for normal lung homeostasis but also for the regeneration of the lung epithelium after, for example, infections. The stem cell properties of AT2 cells are particularly important here (Juil et al. 2020). Thus, various studies have investigated how mesenchymal cells regulate the proliferation and differentiation of lung epithelial



© The Author(s) 2024. **Open Access** This article is licensed under a Creative Commons Attribution 4.0 International License, which permits use, sharing, adaptation, distribution and reproduction in any medium or format, as long as you give appropriate credit to the original author(s) and the source, provide a link to the Creative Commons licence, and indicate if changes were made. The images or other third party material in this article are included in the article's Creative Commons licence, unless indicated otherwise in a credit line to the material. If material is not included in the article's Creative Commons licence and your intended use is not permitted by statutory regulation or exceeds the permitted use, you will need to obtain permission directly from the copyright holder. To view a copy of this licence, visit <http://creativecommons.org/licenses/by/4.0/>.

cells (Yao et al. 2024; Kathiriya et al. 2022; Murthy et al. 2022; Alysandratos et al. 2022; Lee et al. 2017; Tsukui et al. 2024; Barkauskas et al. 2013; Zepp et al. 2017) and, conversely, how epithelial cells influence fibroblasts (Yao et al. 2024; Murthy et al. 2022; Lee et al. 2017; Ushakumary et al. 2021). For example, at least in mice, fibroblasts mediate the growth, self-renewal and differentiation of AT2 progenitor cells via the wingless-related integration site (WNT)-, fibroblast growth factors (FGF)- and IL-6/activator of transcription-3 (STAT3)-regulated ways (Yao et al. 2024; Lee et al. 2017; Zepp et al. 2017; Ushakumary et al. 2021; Riccetti et al. 2020). A central role of the Wnt and Fgf pathways has also been demonstrated in the differentiation of AT2 cells in interaction with fibroblasts in human organoids and by analysis of patient samples (Zacharias et al. 2018; Aros et al. 2021; Jacob et al. 2017; Konigshoff et al. 2009).

However, defective AT2 and mesenchymal cells are also associated with the pathogenesis of chronic lung disease such as chronic obstructive pulmonary disease (COPD) and idiopathic pulmonary fibrosis (IPF). These diseases are characterized by a massive loss of lung function and are incurable. In IPF, scarring of the lungs occurs due to fibrotic, overactivated fibroblasts and a loss of pneumocytes (Ushakumary et al. 2021; Parimon et al. 2020; Tsukui et al. 2020). COPD is characterized by chronic pulmonary inflammation and parenchymal destruction leading to emphysema (Guarnier et al. 2023). It is likely that fibroblasts contribute to the ongoing inflammation in the lungs of COPD patients by secreting inflammatory and senescence-related factors (Woldhuis et al. 2021; Ghonim et al. 2023). However, the extent to which impaired fibroblast interaction with AT2 cells leads to lung parenchymal loss remains unclear.

The occurrence of IPF is associated with a variety of risk factors, including genetic risks such as certain MUC5B promoter variants, environmental exposures (e.g. smoking, viral infections), and aging (Michalski and Schwartz 2020). Repeated microinjuries to the alveolar epithelium are thought to play a role in the development of IPF. These injuries potentially contribute to impaired communication between epithelial cells and fibroblasts, leading to activation and proliferation of misdirected fibroblasts, accumulation of large amounts of extracellular matrix (ECM), remodeling of the ECM, cellular senescence, and destruction of the lung epithelium (Martinez et al. 2017). Signaling pathways important for normal lung homeostasis, such as Wnt-signaling, are thought to play a critical role in the progression of IPF when imbalanced (Aros et al. 2021; Ye and Hu 2021).

The aim of the present study was to analyze the interaction of primary human fibroblasts and AT2 cells in an organoid model. We show that co-cultivation of AT2 organoids with fibrotic fibroblasts leads to STAT3

activation and aberrant secretory activity characterized e.g. by MUC5B. Fibroblasts express factors that activate STAT3 pathways in AT2 cells and IL-6 induces cystic growth of the organoids.

Results

Co-culture with fibroblasts leads to cystic growth of the organoids

To investigate the impact of fibroblasts on alveolar organoid differentiation, we isolated AT2 cells and differentiated them in co-culture with primary fibroblasts for 21 days or control media (Fig. 1a). Immunostaining confirmed the AT2 identity of the cells as well as the absence of the airway epithelial markers KRT5 and CCSP (S1). Co-cultivation with fibroblasts significantly influenced the morphology of the organoids. In the absence of fibroblasts, more than 95% of the organoids showed a grape-like growth, while organoids cultured with fibroblasts had a cystic morphology (Fig. 1b and c). This was accompanied by an increased diameter of the organoids co-cultured with fibroblasts (Fig. 1d). Co-culture with the fibroblast cell line MRC5 led to larger organoids, but not to a cystic growth comparable to primary fibroblasts (S2).

Fibroblasts induce a secretory phenotype in alveolar type-2 cells

Next, we characterized alveolar organoids in co-culture with fibroblasts obtained from three different donors for 21 days by scRNA sequencing using BD Rhapsody™ Single-Cell Analysis System. Representative markers (Sikkema et al. 2023) showed that the cultures were composed of epithelial cells (EPCAM) and fibroblasts (COL1A1), with the fibroblasts only being found in co-cultures (S3). The fibroblasts expressed typical fibroblast markers, high levels of collagens as well as markers specifically produced by fibrotic fibroblasts such as CTHRC1, SERPINH1 and TNFRSF12A (Fig. 2) (Tsukui et al. 2024; Peyser et al. 2019; Herrera et al. 2022; Guo et al. 2024). Since the fibroblasts were isolated from disease-free regions of the lung (F1: lung cancer; F2: lung cancer with COPD; F3: pulmonary fibrosis), the phenotype of the fibroblasts is model-related and independent of the donor.

For further analysis, we sub-clustered the epithelial cells and identified 4 clusters: AT2 cells, aberrant AT2 cells, proliferating AT2 cells, and dedifferentiated cells (Fig. 3a to c). Aberrant AT2 showed reduced expression of SFTPC, while other type 2 markers such as NAPSA and LAMP3 were increased. In addition, aberrant AT2 expressed secretory factors such as MUC5B and CXCL8. Dedifferentiated cells showed low expression for SFTPC and high expression for SFTPB and SCGB3A2 and resembled the recently discovered human terminal and respiratory bronchiole secretory cells (TRB-SCs)

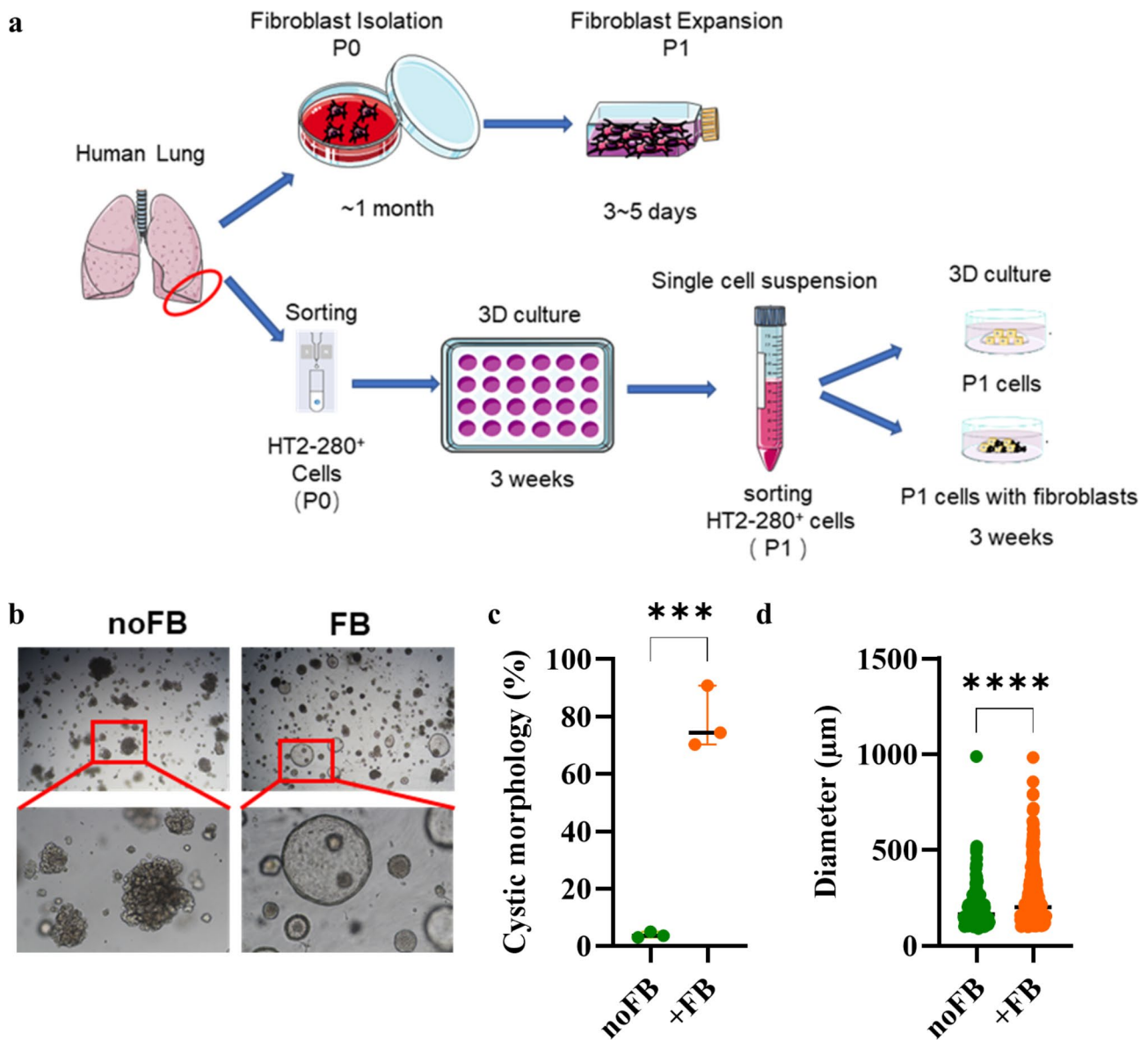


Fig. 1 Fibroblasts induce cystic organoid growth. **(a)** Scheme of the experimental layout. **(b)** Representative phase contrast images of organoids cultured for 21 days (noFB: AT2 cells cultured without fibroblasts (FB); FB: AT2 cells cultured in the presence of fibroblasts, P1: passage 1). **(c)** Quantification of the morphology of the alveolar organoids. Data were compared by unpaired t-test ($***p < 0.001$). Each data point represents an independent experiment. **(d)** Quantification of the diameter of the alveolar organoids. Pooled results from 3 independent experiments. Data were compared by Mann-Whitney test ($****p < 0.0001$)

, which can differentiate from AT2 cells (Fig. 3c and d, S4a/b) (Murthy et al. 2022). Co-culture with fibroblasts resulted in a shift from AT2 cells to aberrant AT2 cells (Fig. 3e, S4c). The epithelial clusters were largely negative for airway epithelial markers such as S100A2, KRT5, and CYP2F1 (S4a/b) (Sikkema et al. 2023). Trajectory analysis for both groups (with and without fibroblasts) showed that proliferating cells differentiated in two directions: AT2 and dedifferentiated cells (Fig. 3f). Together, these results indicate that fibroblasts drive AT2 cells towards MUC5B-expressing AT2-like cells in this model.

Fibroblasts induce expression of MUC5B in pneumocytes

Immunofluorescence microscopy and semi-quantitative RT-PCR analyses showed, in addition to the single cell analyses, that the co-culture with fibroblasts from all three donors led to a reduced expression of SFTPC and a significantly increased expression of MUC5B (Fig. 4a to c, also Fig. 5d). Increased expression of MUC5B was not present in co-cultures with MRC5 cells (S2C). However, co-culture with MRC5 cells results in a decreased expression of SFTPC and thus in a loss of AT2 identity (S2C). Consistent with the single cell analysis, the organoids

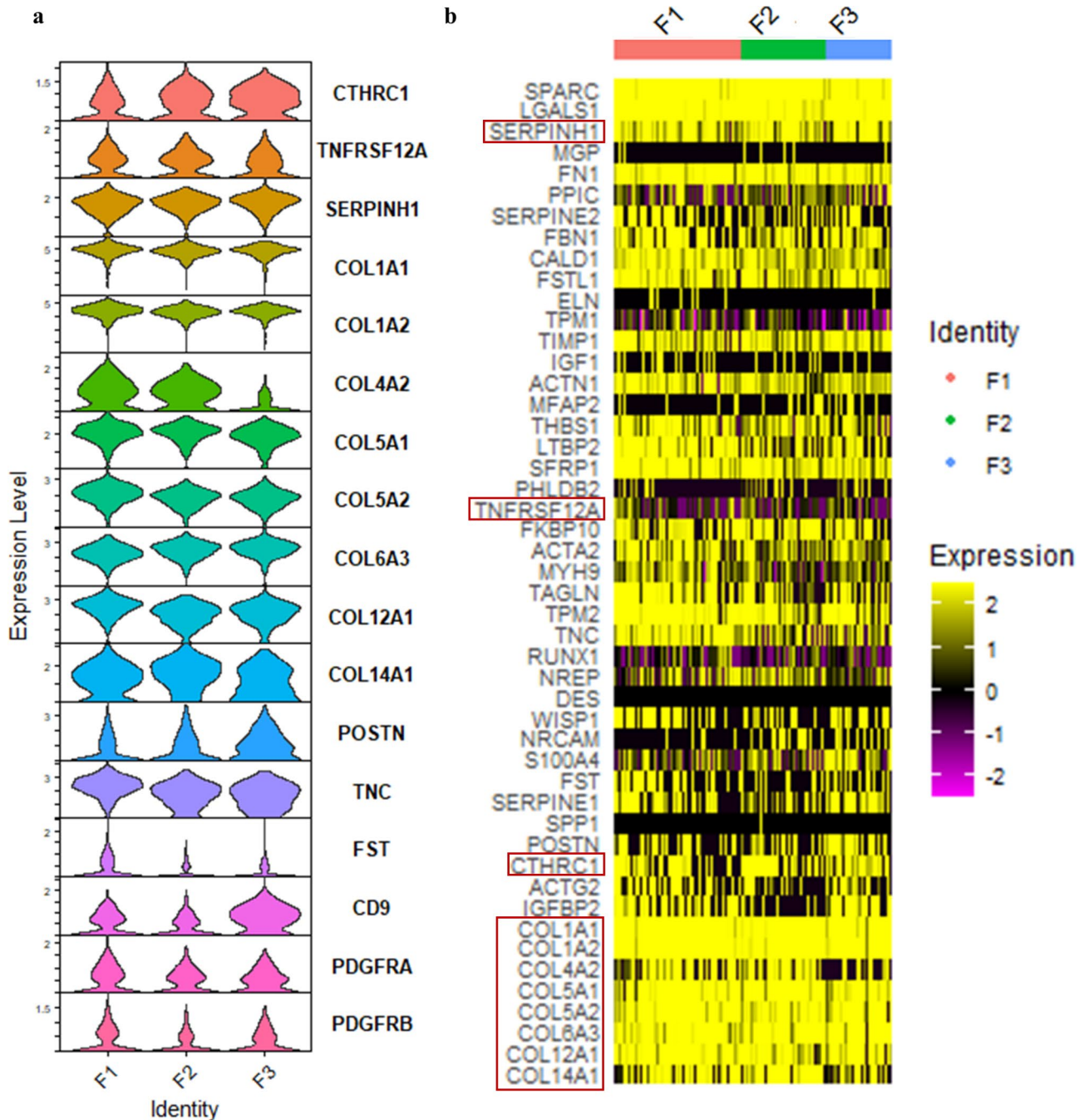


Fig. 2 Fibroblasts show a pro-fibrotic phenotype. **(a)** Violin plots showing the expression levels of fibrosis markers for the three donors (F1-3). **(b)** Heat-map for markers of pathogenic fibroblasts. Key pro-fibrotic genes are highlighted

were negative for the airway epithelial markers KRT5 and SCGB1A1 (Fig. 4D).

Staining of lung tissue from IPF patients showed strong expression of MUC5B in fibrotic lesions partially associated with SFTPC-expressing cells (Fig. 5, S5). Re-analysis of the single-cell data published by Habermann et al. (Habermann et al. 2020) revealed around 25% of MUC5B-expressing cells in the AT2 cell cluster of IPF patients (S6).

IL-6-STAT3 signaling drives MUC5B-expression in AT2 cells

Gene set variation analysis (GSVA, Fig. 6a, S7a) and AUCell (Fig. 6b, S7b) showed that IL-6/STAT3 and TNF- α /NF κ B pathways were activated in aberrant AT2 cells. The PI3K-Akt signaling pathway was strongly activated in fibroblasts (S7C). IL-6 concentrations were increased in supernatants from co-cultures with primary fibroblasts (Fig. 6c) and fibroblasts, but not epithelial cells expressed IL-6 (Fig. 6d). STAT3 was highly expressed and

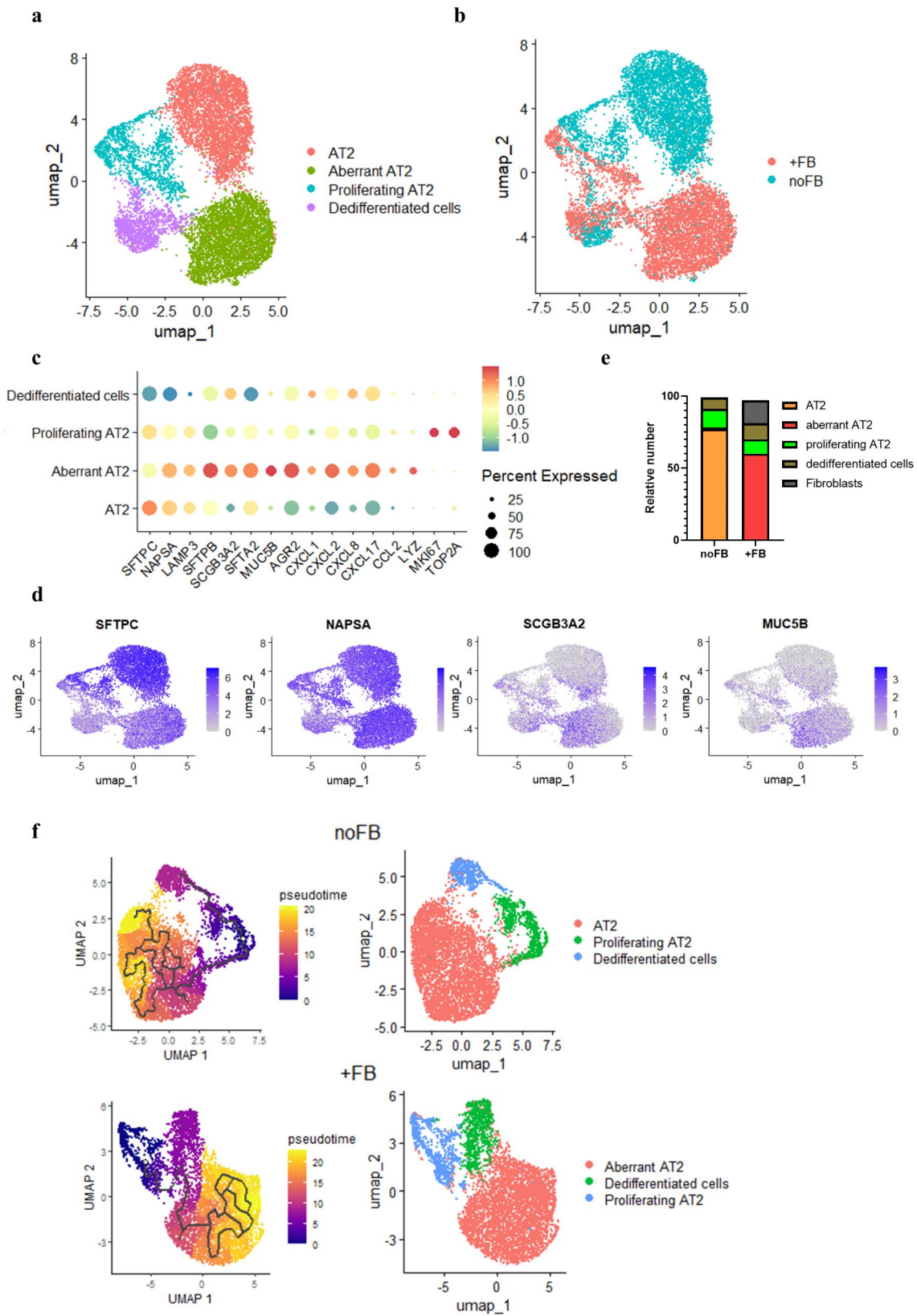


Fig. 3 Fibroblasts drive the differentiation of AT2 cells toward a secretory phenotype. **(a)** UMAP visualization of different cell types. **(b)** UMAP visualization colored by groups (noFB: AT2 cells cultured without fibroblasts; +FB: AT2 cells cultured in the presence of fibroblasts). **(c)** Dot plot showing expression of epithelial cell type markers and secretory factors markers. **(d)** Feature plots showing the expression of representative markers for AT2 and secretory cells. **(e)** Proportion of the different cell clusters. **(f)** Pseudotime trajectory analysis by Monocle 3 of the two groups

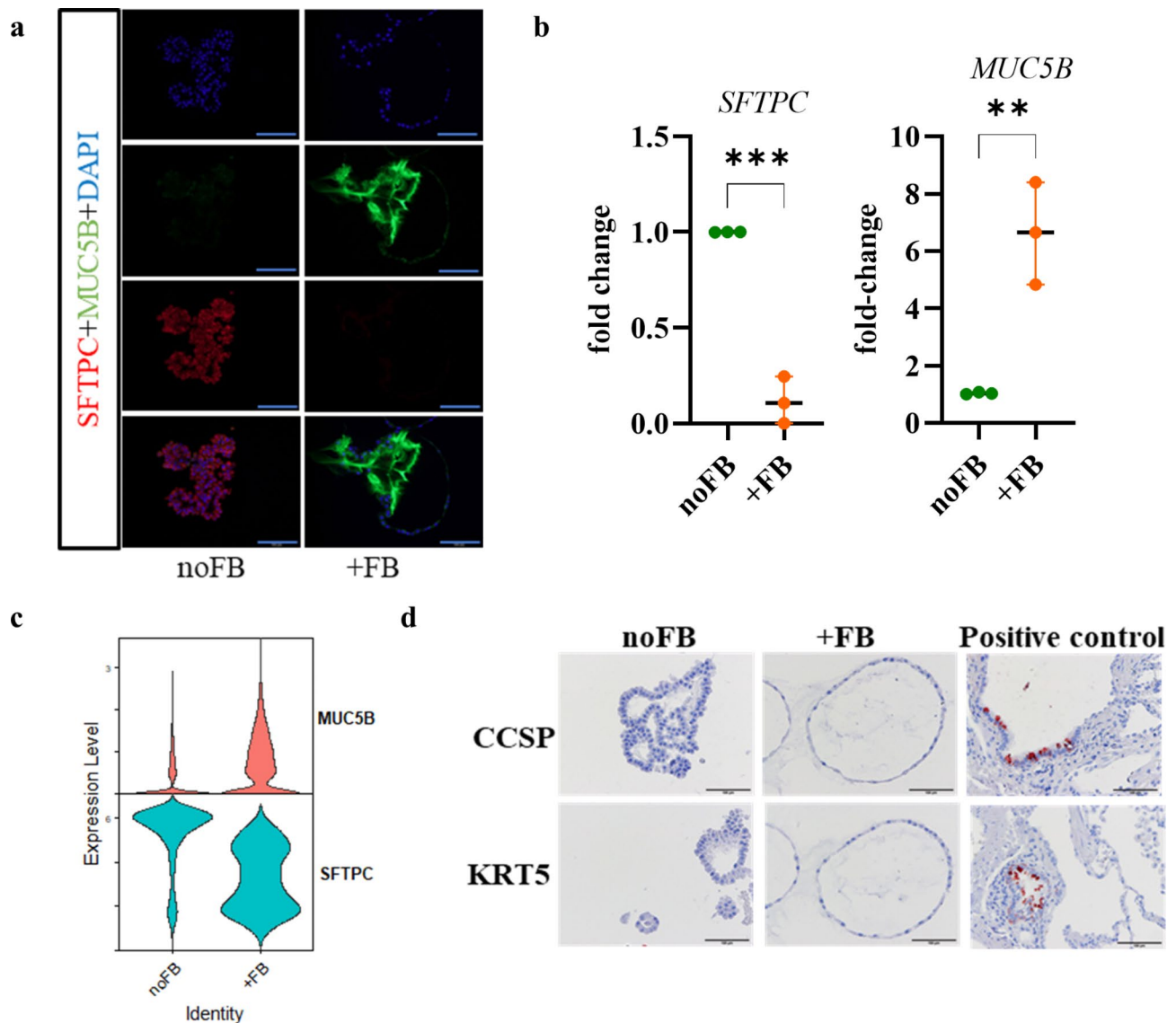


Fig. 4 Fibroblasts induce the expression of MUC5B. **(a)** Organoids were stained for SFTPC and MUC5B by immunofluorescence (Scale bar = 100 μ m). **(b)** The expression of SFTPC and MUC5B was confirmed by semi-quantitative RT-PCR. Data were compared by unpaired t test (** $p < 0.01$, *** $p < 0.001$). Each data point represents an independent experiment. **(c)** Violin plots showing expression of SFTPC and MUC5B. **(d)** Immunohistochemistry was performed for CCSP and KRT5 (positive control: human lung tissue; scale bar = 100 μ m)

phosphorylated in nuclei of pneumocytes cultured with fibroblasts (Fig. 6d and e). Staining of lung tissue from IPF patients showed expression of IL-6 in fibrotic lesions partially associated with PGFRA-expressing cells (S8).

As fibrotic fibroblasts express IL-6 and induce IL-6-STAT3 signaling (Fig. 6, S9), we examined, whether ongoing stimulation with IL-6 affects the phenotype of organoids. Stimulation with IL-6 from the day of seeding resulted in a cystic, MUC5B-expressing phenotype with nuclei positive for phosphorylated STAT3. IL-6 decreased the expression of SFTPC, but not NAPSA (Fig. 7, S10).

In order to take a closer look at the interaction of the fibroblasts with the pneumocytes, ligand-receptor

analysis was carried out for the pneumocyte-fibroblast co-cultures. Fibroblasts expressed HGE, TWEAK (TNFSF12) and PTN with predicted receptivity in the pneumocytes (Fig. 8a and b, S11a). Autocrine and paracrine induction of LIF/LIFR signaling, which has been shown to mediate IL-6 expression in fibroblasts (Nguyen et al. 2017), is predicted in fibroblasts (Fig. 8A, S11a and b). GDF15 expressed by epithelial cells (Fig. 8b, S11c) is predicted to signal from pneumocytes to fibroblasts (Fig. 8a and c). Primary fibroblasts, but not the cell line MRC5 expressed increased levels of IL-6 in response to GDF15 and LIF (Fig. 8d). Together, our data suggest that prolonged release of STAT3-activating factors by fibroblasts results in aberrant secretory AT2 cells that further

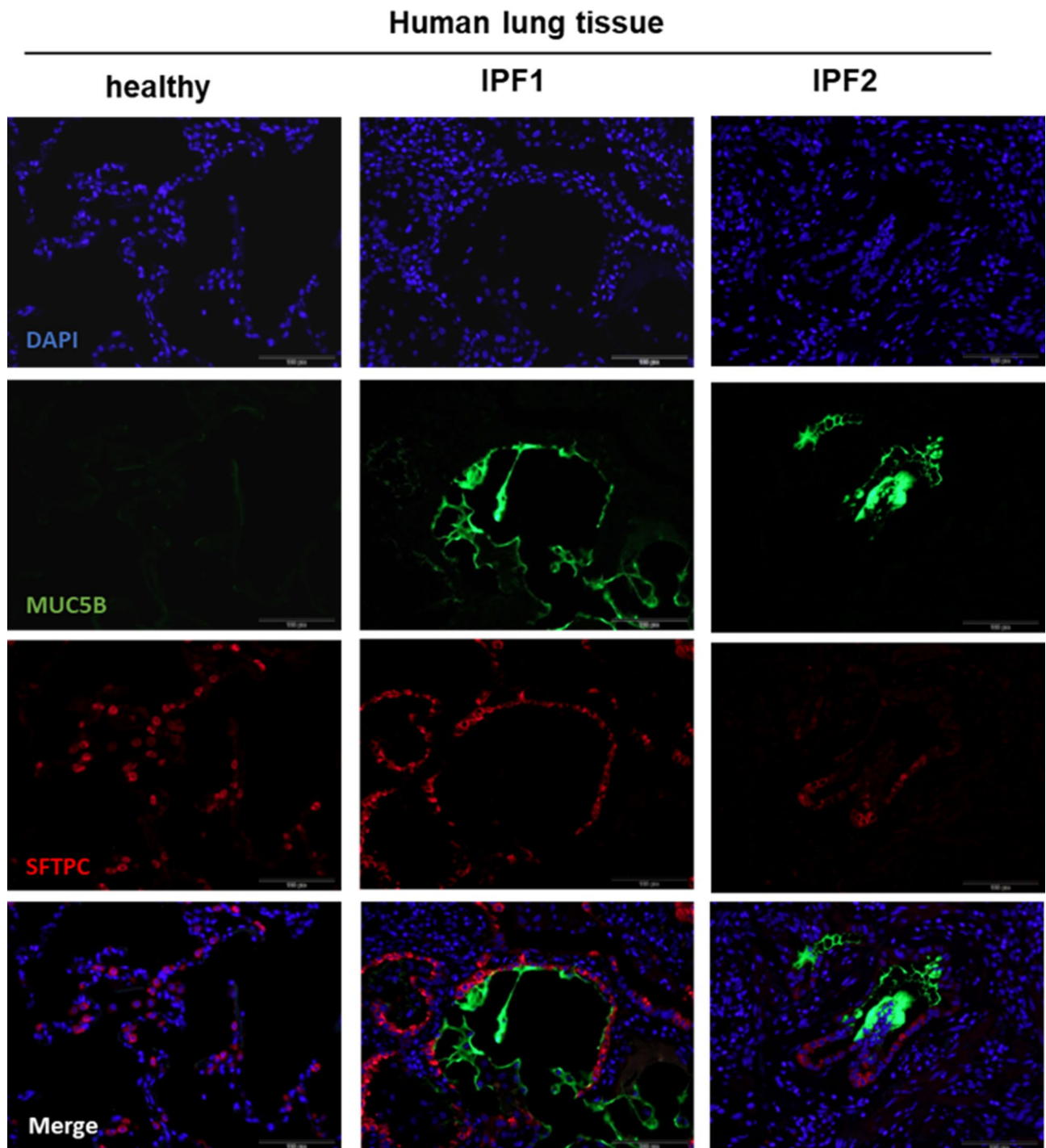


Fig. 5 Strong expression of MUC5B in fibrotic lesions in lungs of IPF patients. MUC5B and SFTPC were detected by immunofluorescence in human lung samples obtained from a healthy donor and two IPF patients (scale bar = 100 μ m)

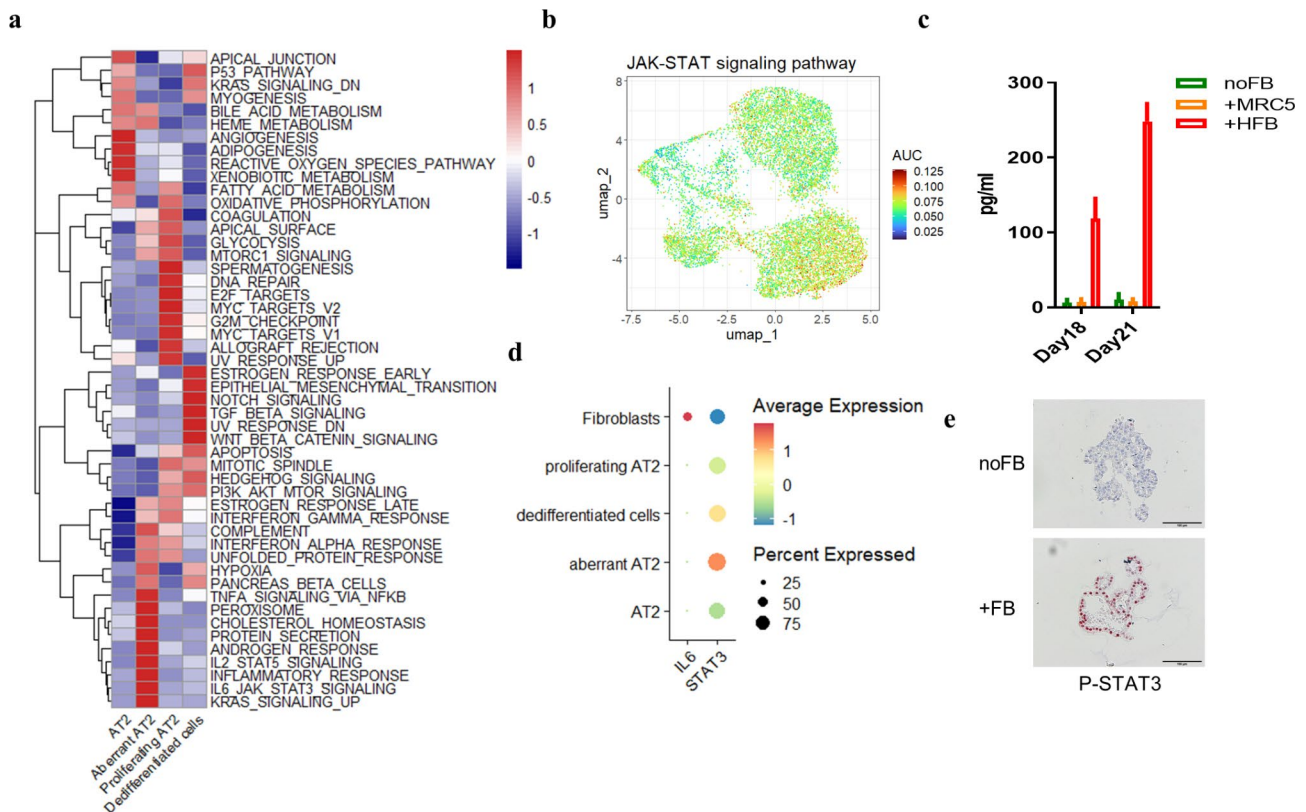


Fig. 6 Fibroblasts activate IL-6/STAT3 pathways. Signaling pathways were analyzed by (a) GSEA and (b) AUCCell. (c) IL-6 was measured in supernatants of the cultures at day 18 and 21. (d) Dot plot showing expression of IL-6 and STAT3. (e) Immunohistochemistry was performed for P-STAT3 (scale bar = 100 μm)

increase IL-6 expression via epithelial factors such as GDF15 (Fig. 8E).

Treatment with dasatinib reduces the formation of mucoid organoids

The single cell analyzes showed that the fibroblasts express markers for senescence and revealed activation for the PI3K-Akt signaling pathway (S7c, S12) (Saul et al. 2022; Moiseeva et al. 2023; Kohli et al. 2021). Using dasatinib (Zhu et al. 2015), we tested to what extent our model can be used to test drugs that counteract the secretory phenotype induced by fibrotic fibroblasts. For this purpose, we pretreated the fibroblasts of the three donors with dasatinib or control medium. Subsequently, co-cultures were established, with dasatinib still being added to the cultures with pretreated fibroblasts. In cultures without fibroblasts, dasatinib had no effect on grape-like morphology and organoid diameter. In contrast, treatment with dasatinib prevented the cystic growth of the organoids in the co-culture (Fig. 9a to c). In dasatinib-treated cultures, MUC5B expression was significantly reduced (9d, S13). However, dasatinib did not reverse the fibroblast-induced loss of SFTPC expression, but did reduce STAT3 phosphorylation (S13).

Discussion

Here, we investigated the influence of primary fibroblasts on the differentiation of AT2 cells in our organoid model. We show that culturing AT2 cells in the presence of fibrotic fibroblasts results in secretory cystic organoids with reduced expression of SFTPC but increased expression of MUC5B. We identified regulatory circuits in which fibroblasts secrete inflammatory mediators such as IL-6 and activate pneumocytes, for example, via STAT3-dependent signaling pathways. We also demonstrate that the model is suitable for studying pharmacological interventions.

Our organoid model reveals high plasticity of AT2 cells, especially when cultured with mesenchymal cells. With a strong expression of SFTPB and SCGB3A2, low expression of SFTPC and no expression of SCGB1A1, the dedifferentiated cells resemble the recently described AT0 and terminal and respiratory bronchiole (TRB) secretory cells, which can differentiate from AT2 cells during lung regeneration (Murthy et al. 2022; Sikkema et al. 2023). In the presence of activated fibroblasts, the pneumocytes cells strongly lost the AT2 identity and developed a pronounced secretory phenotype.

A high plasticity of AT2 cells was also demonstrated by Kathiriya et al. in organoid models (Kathiriya et al.

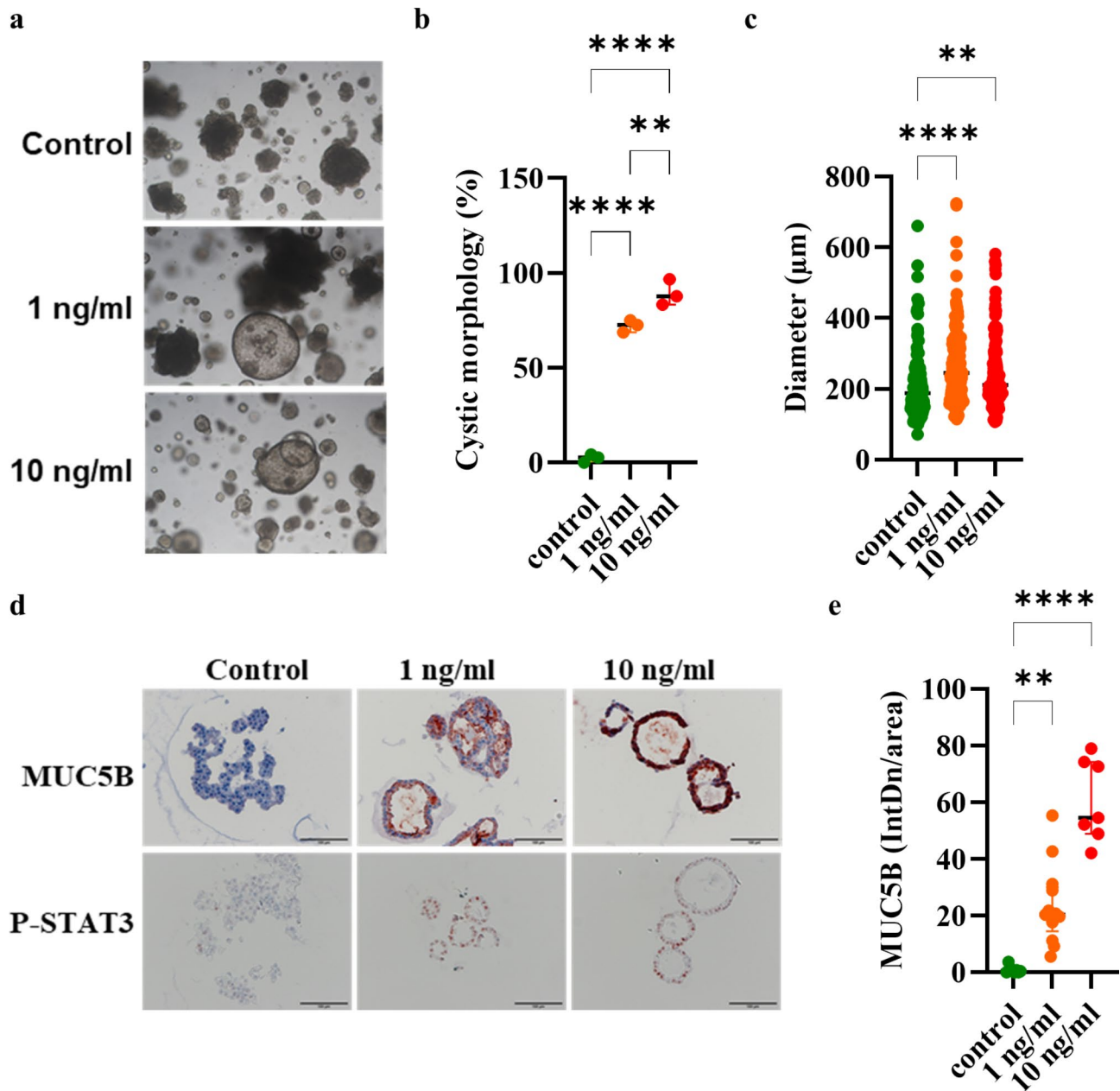


Fig. 7 IL-6 induces the differentiation of AT2 cells towards a MUC5B⁺ cystic phenotype. The organoid cultures were stimulated with IL-6 from the day of seeding. **(a)** Representative phase contrast images of organoids cultured for 21 days. **(b)** Quantification of the morphology of the alveolar organoids. **(c)** Quantification of the diameter of the alveolar organoids. **(d)** Immunohistochemistry was performed for MUC5B and P-STAT3 (scale bar = 100 μm). **(e)** Quantification of MUC5B staining. Data were compared by one-way ANOVA (** $p < 0.01$, **** $p < 0.0001$)

2022). The authors showed that human AT2 cells, but not murine AT2 cells, transdifferentiate into basaloid cells when cultured in the presence of activated mesenchymal cells. Unlike the basaloid cells, the aberrant AT2 cells in our model did not show any expression of markers for airway epithelial cells such as KRT5 (Kathiriya et al. 2022; Adams et al. 2020). The differences between our study and Kathiriya et al. could be result from the different culture media used. The WNT-activator used in our study might prevent the differentiation of AT2 cells to KRT5⁺

basal cells. In our model there was also no evidence of intermediate steps, such as KRT17⁺/KRT8^{High} cells (S4) (Kathiriya et al. 2022), on the transdifferentiation pathway. Rather, there was a continuum from SFTPC-expressing to MUC5B-expressing cells. Future studies must show to what extent fibroblasts modulate the differentiation of AT2 cells towards a secretory phenotype in chronic lung diseases such as IPF, without further differentiation into basaloid cells.

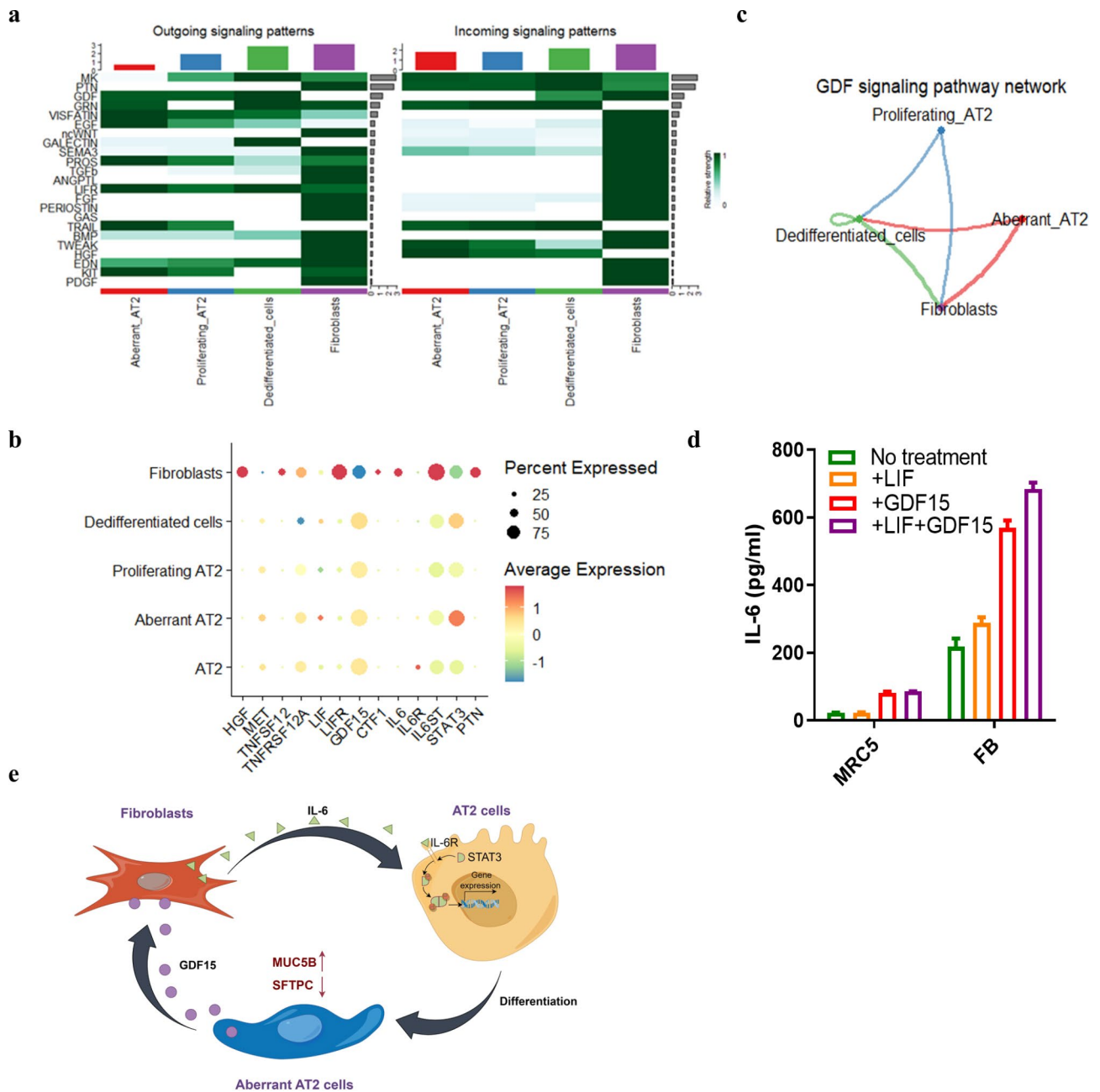


Fig. 8 Fibroblasts activate IL-6/STAT3, TNF- α and HGF pathways in aberrant AT2 cells. **(a)** Heatmap (prediction of the CellChat algorithm) with outgoing and incoming signals in the different cell types. **(b)** Dot plot showing expression of selected ligands and receptors. **(c)** Signaling activity of GDF15 between epithelial cells and fibroblasts predicted by CellChat algorithm. **(d)** Primary fibroblasts and the cell line MRC5 were incubated for 24 h with GDF15 (200 ng/ml) and LIF (100 ng/ml) and IL-6 concentrations were measured in the supernatants. **(e)** Proposed schematic diagram of fibroblast-epithelial cell interaction.

The secretory aberrant AT2 cells in our model expressed MUC5B. MUC5B is typically produced by airway epithelial cells such as goblet cells and not by pneumocytes (Sikkema et al. 2023). Numerous preclinical and clinical studies indicate an important role of MUC5B in the pathogenesis of IPF. MUC5B promoter variants are a dominant risk factor for the development of IPF (Moore et al. 2019; Borie et al. 2013, 2022; Seibold et al. 2011;

Fingerlin et al. 2013; Zhang et al. 2011; Stock et al. 2013; Peljto et al. 2015). Furthermore, MUC5B is abundantly expressed in honeycomb cysts, which are characteristic structures in fibrotic lesions, as well as in the distal airways of IPF patients (Conti et al. 2016; Hancock et al. 2018). We also could detect a strong MUC5B expression which partially associated with SFTPC⁺ cells. Hancock et al. showed that, in IPF patients, MUC5B is co-expressed

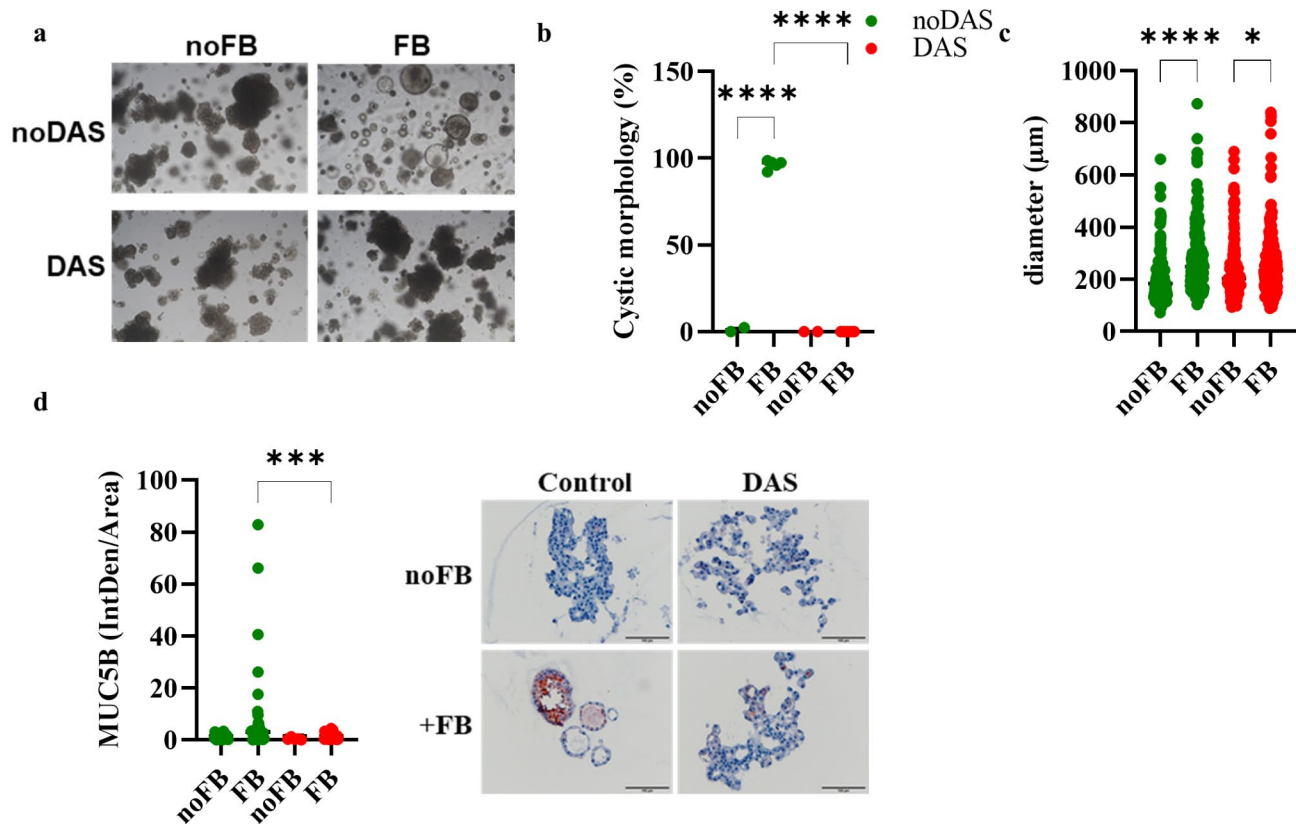


Fig. 9 Dasatinib reduces cystic organoid formation. The organoid cultures were incubated with dasatinib (200 nM) from the day of seeding. **(A)** Representative phase contrast images of organoids cultured for 21 days. **(B)** Quantification of the morphology of the alveolar organoids. Each data point represents an independent experiment. **(C)** Quantification of the diameter of the alveolar organoids. **(D)** Immunohistochemistry was performed for MUC5B (scale bar = 100 µm). **(E)** Quantification of MUC5B staining. Pooled results from 3 independent experiments. Data were compared by one-way ANOVA (* $p < 0.05$, *** $p < 0.01$, **** $p < 0.0001$)

with SFTPC in epithelial cells lining the honeycomb cyst and in AT2 cells, suggesting that epithelial cells in the lung parenchyma express MUC5B in IPF (Hancock et al. 2018). Forced expression of *Muc5B* under the control of the *Sftpc* promoter in the distal lung worsened the outcome in the bleomycin-induced mouse model (Hancock et al. 2018; Kurche et al. 2019). Although numerous cell types in the IPF lung likely contribute to deleterious expression of MUC5B, our results suggest that fibrotic fibroblasts drive AT2 cells toward MUC5B-expressing AT2 cells, as described for honeycomb cysts (Conti et al. 2016; Hancock et al. 2018).

Our single-cell data showed that the fibroblasts in the co-culture model adopted an IPF-like phenotype, similar to fibroblasts in IPF lungs and the mouse fibrosis model (Kathiriya et al. 2022; Peyser et al. 2019; Adams et al. 2020; Jia et al. 2023). The analysis also showed that fibroblasts activate signaling pathways (e.g. STAT3-, NFκB-, and HGF-dependent pathways) in pneumocytes that have a strong influence on cell differentiation. Conversely, pneumocytes had an influence on signaling pathways (e.g. LIF/LIFR signaling) related to the expression of IL-6 in fibroblasts (Nguyen et al. 2017). In vitro and mouse

studies suggest that IL-6 released by fibroblasts promotes AT2 self-renewal and lung regeneration through STAT3-signaling (Zepp et al. 2017; Liang et al. 2016; Yao et al. 2023; Paris et al. 2020). However, IL-6-STAT3 signaling has been shown to play a central role in murine pulmonary fibrosis models (Le et al. 2014; O'Donoghue et al. 2012; Pedroza et al. 2016) and phosphorylated STAT3 was detected in nuclei of pneumocytes next to fibrotic lesions in the lungs of IPF patients (Pedroza et al. 2016). Thus, it is conceivable that an out-of-control activation of signaling pathways that are initially important for pneumocyte regeneration, such as IL6/STAT3-signaling, leads to a dysregulated pneumocytes with a secretory pneumocyte.

Our finding that profibrotic fibroblasts cause loss of AT-2 identity is also supported by further ex vivo studies showing that treatment of precision-cut lung slices (PCLS) and organoids with a fibrosis cocktail leads to reduced expression of AT-2 markers such as SFTPC (Alsafadi et al. 2017; Ptasinski et al. 2023; Lehmann et al. 2018). Kastlmeier showed that pluripotent stem cell-derived organoids lose AT2 identity when co-cultured with lung fibroblasts from fibrotic ILD patients

(Kastlmeier et al. 2023). Bleomycin- and H₂O₂-treated human fibroblasts also reduced the progenitor potential of alveolar epithelial stem cells in the organoid model (Melo-Narvaez et al. 2024). Thus, organoid models depict aspects of disease and are therefore suitable for testing pharmacological compounds, especially in preclinical research before animal experiments (Brand et al. 2024).

Senescence is thought to play a role in the pathogenicity of chronic lung disease (Barnes et al. 2019; Hamsanathan et al. 2019). Our single cell analyzes showed strong expression of markers associated with senescence (e.g. CDKN2A, TIMP2, IL-6) and activation of the PI3K-Akt signaling pathway in fibroblasts. Thus, to test whether our model is suitable for pharmacological interventions, we treated the cultures with the drug dasatinib, which, among other things, is considered a senolytic agent that acts on the PI3K signaling pathway (Chaib et al. 2022). Dasatinib treatment resulted in increased expression of SFTPC and decreased expression of MUC5B in cultures lacking fibroblasts. Furthermore, dasatinib counteracted the cystic phenotype and fibroblast-induced expression of MUC5B without leading to an AT2 phenotype comparable to cultures without fibroblasts, at least with respect to the expression of SFTPC. Further studies are needed to elucidate the exact mechanism of action of agents such as dasatinib and other approved drugs (e.g. metformin) as well as natural compounds in relation to impaired pneumocyte differentiation and the formation of the recently discovered basaloid cells (Kathiriya et al. 2022; Adams et al. 2020; Jaeger et al. 2022). Moreover, the question arises to what extent the expression of MUC5B contributes significantly to pulmonary fibrosis and whether drugs that suppress the expression of MUC5B are helpful. Cell culture models, such as ours, can undoubtedly make a significant contribution to the testing of active ingredients with respect to their effects on diverse cell types and cellular mechanisms within the human system.

Based on the activation status of the included cells, our organoid model has limitations. Fibroblasts are highly activated in such models (Kathiriya et al. 2022; Melo-Narvaez et al. 2024), probably because they activate different pathways, such as repair programmes, in this unnatural environment. The required expansion of patient-derived fibroblasts for one to two weeks in conventional 2D culture also induces a fibrosis-like phenotype (Habermann et al. 2020). It is therefore almost impossible to introduce fibroblasts into 3D co-culture models as they exist in the donor lung, and difficult to study the extent to which fibroblasts from healthy and diseased tissue differ. However, the model allows direct assessment of pro-fibrotic activity without the need for exogenous application of additional fibrosis-inducing factors such as a fibrosis cocktail (Alsafadi et al. 2017; Ptasinski et al. 2023; Lehmann et al. 2018). Moreover, the medium contains several

components (e.g., the WNT activator CHIR99021) that can affect fibroblast behavior in a complex manner, such as the release of growth and fibrotic factors. Due to donor variability, independent experiments with cells from different donors should always be performed in complex models using primary cells for drug testing. The complex isolation and cultivation of primary organoids is a significant additional effort in comparison to cell line models and conventional 2D cultures.

In summary, our results show that activated fibroblast induce a secretory phenotype characterized by MUC5B expression in AT2 organoids. Remarkably, this was not accompanied by the expression of respiratory epithelial markers. Excessive fibroblast-induced activation of signaling pathways associated with epithelial regeneration leads to a pathogenic AT2 phenotype in our model, as might also be the case in chronic lung diseases such as IPF. The model is well suited for testing active ingredients, e.g. in pre-clinical research.

Materials and methods

Sex as a biological variable

Sex was not considered as a biological variable.

Human lung alveolar epithelial cell isolation and sorting

Alveolar epithelial cells were isolated from surgically removed lung tissue from the patient. The protocol for human material has been approved by the Landesärztekammer des Saarlandes Ethics Committee and informed consent has been obtained from all patients. The tissue was cut into small pieces and digested with a digestion solution containing 2.5 mg/ml collagenase type I (Life technologies, 17100-017), 1 ml dispase (Corning, 354235), 1 mg/ml DNase1 (Roche, 10104159001) for 35 min at 37 °C. The obtained cell suspension was filtered through a 70 µm cell strainer and centrifuged at 450 x g for 10 min at 4 °C. The red blood cells were then lysed with ACK buffer (Gibco, A1049201), and the remaining cells were washed twice with PBS containing 1% FBS (Gibco, 10270106), 1 mM EDTA (Roth, 8043.2). Then, HT2-280⁺ cells were obtained by incubating with HT2-280 antibody (Terrance, TB-27AHT2-280) for 1 h and afterwards with anti-mouse IgM beads (Miltenyi, 130-047-302) for 30 min in the dark at 4 °C. Labeled cells were sorted by MACS column (Miltenyi).

Human lung fibroblasts isolation and culture

Lung (~ 1 cm³) tissue was cut into 6–8 individual pieces and cultured in petri dishes in DMEM medium (Gibco, 41965039) containing 10% FBS and 1% penicillin/streptomycin (Gibco, 1514). Media were changed every 4 days. Once the fibroblasts reached 80–90% confluence, cells were stored at -80 °C for future use.

Human AT2 organoid culture and assay

AT2 organoid cultures were cultivated as described previously (Katsura et al. 2020). Briefly, HT2-280⁺ cells were resuspended in GFR-Matrigel and 5 × 10³ cells were seeded in each well of a 24-well plate. After 30 min of incubation at 37 °C to solidify the Matrigel, cells were cultured for 21 days with 500 μL of Advanced DMEM/F12 medium (Thermo Fisher Scientific, 12634010) containing 10 μM SB431542 (Abcam, Ab120163), 3 μM CHIR99021 (Tocris, 4423), 1 μM BIRB796 (Tocris, 5989), 50 ng/mL human EGF (Gibco, PHG0313), 10 ng/mL human FGF10 (BioLegend, 559304), 5 μg/mL heparin (Sigma-Aldrich, H3149), 1x B-27 supplement (Thermo Fisher Scientific, 17504044), 1x antibiotic-antimycotic (Gibco, 15240062), 15 mM HEPES (Thermo Fisher Scientific, 15630080), 1x GlutaMAX (Thermo Fisher Scientific, 35050061), and 1.25 mM N-acetyl-L-cysteine (Sigma-Aldrich, A9165). 10 μM of Y-27,632 (Sigma-Aldrich, Y0503) was added on the first 3 days of culture. The medium was changed every 3 days. For passaging, Matrigel was disrupted by incubation with dispase at 37 °C for 45 min, followed by single cell dissociation through the addition of TrypLE™ Express Enzyme (Gibco, 12605010) for 5 min at 37 °C. The cells were centrifuged at 450 x g for 5 min and resuspended in fresh GFR-Matrigel as before. In co-culture experiments, HT2-280⁺ and human lung fibroblasts were cultured in GFR-Matrigel at a 1:1 ratio for 21 days. In the IL-6 (PeproTech, 200-06-20UG) and Dasatinib (BMS-354825) experiments, 1 ng/ml or 10 ng/ml of IL-6 and 200 nM of Dasatinib were added to the medium for 21 days, respectively.

Immunofluorescence (IF) and immunohistochemistry (IHC) staining

Organoids were embedded with 3% agarose as described before (Brand et al. 2024; Sprott et al. 2020). Primary antibodies for pro-SFTPC (Abcam, ab90716, 1/100) and MUC5B (Santa Cruz Biotechnology, sc-393952, 1/100) were used in IF staining. Primary antibodies for pro-SFTPC (1/5000, ab90716), MUC5B (1/500, sc-393952), KRT5 (1/1000, ab75869), NAPSA (1/1000, ab133249), CCSP (1/2000, ab307666) and STAT3 (1/500, 9145 S) were used in IHC staining. MUC5B staining intensity was quantified using ImageJ (National Institutes of Health, Bethesda, MD, USA) software and related to the area occupied by the organoid.

qRT-PCR

Gene expression levels were quantified by qRT-PCR on the CFX 96™ Real-Time PCR Detection System (Bio-Rad) as described previously (Yao et al. 2024). Primers are listed in Table 1 in the online supplement.

Single cell sequencing analysis

Organoids were digested into single cells using the methods described for passaging. Single cell analysis was performed using the BD Rhapsody™ Single-Cell Analysis System (Becton Dickinson, San Jose, CA, USA) according to manufacturer's protocols. Samples were individually labelled using the Human Single-Cell Multiplexing Kit (BD, Cat. 633781) and subsequently pooled. Cells were captured, cell-specific mRNAs were transferred to barcoded capture beads, libraries were generated by use of the BD Rhapsody™ WTA Amplification Kit (BD, Cat. 633801) and finally sequenced on the Novaseq 6000 platform (Illumina, USA) with about 50,000 reads per cell. Raw sequencing reads were processed with the BD Rhapsody™ WTA Analysis Pipeline on the Sevenbridges cloud platform.

Data were processed with the Seurat package (version 5.0.1) in R software (version 4.3.1). Low-quality cells with gene expression < 2000 or > 10,000 genes or the percent of mitochondrial reads over 15% of total reads per cells were filtered out. The filtered dataset was normalized and scaled by using Seurat NormalizeData (scale factor 10,000) and ScaleData function with default parameters. Cell clusters were identified using a shared nearest neighbors (SNN)-based algorithm (resolution was set to 0.3). Nonlinear dimensional reduction was performed to generate UMAP plots as illustrated. GSVA (1.50.0) and AUCell (1.24.0) package in R was used for pathway activities analysis. The gene sets for signaling pathway activities were derived from "KEGG_2021_Human" list. CellChat (1.6.1) was used with default parameters for ligand-receptor interaction analysis. Single-cell pseudotime trajectories were generated with the Monocle3 package (Version 1.3.4) in R (Qiu et al. 2017).

Supplementary Information

The online version contains supplementary material available at <https://doi.org/10.1186/s10020-024-00990-w>.

Supplementary Material 1

Acknowledgements

The authors thank Anja Honecker (Saarland University, Department of Internal Medicine V) for excellent technical support. The authors thank Jörn Walter (Saarland University, Genetics/Epigenetics) for computational resources and advise.

Author contributions

Y.Y.; F.R.: designing research study, conducting experiments, acquiring data, analyzing data, providing reagents, writing the manuscript; F.L.: providing reagents; R.B., C.B.: designing research study, analyzing data, writing the manuscript; K.K.: analyzing data; M.B., C.H., S.M., A.K. and H.G.: conducting experiments, acquiring data, analyzing data. All authors confirm that they had full access to all the data in the study and accept responsibility to submit for publication.

Funding

This study was supported by grants from Dr. Rolf M. Schwiete Stiftung to RB and Eduard Kastner (Stiftung Forschung für Leben) to RB, startup funding of the Saarland University to CB and the German Federal Ministry of Education and Research (BMBF) in the call "Alternative methods to animal experiments" (project 3-REPLACE, 16LW0140K) to CB and DY. Open Access funding enabled and organized by Projekt DEAL.

Data availability

The single cell data is available at: <https://0-www-ncbi-nlm-nih-gov.brum.beds.ac.uk/geo/query/acc.cgi?acc=GSE254441>.

Declarations

Ethics approval and consent to participate

The protocol for isolation of human cells was approved by the Institutional Review Board (ethics committee, Nr-34/18) of the Saarland State Medical Association and informed consent was obtained from the patients.

Consent for publication

Not applicable.

Statistics

Graph Prism software (GraphPad Software (version 8.0), San Diego, CA) was used for statistical analysis. Comparisons between groups were analyzed by one-way ANOVA, unpaired t-test or Mann-Whitney test as indicated in the figure legends. The results were considered statistically significant for $p < 0.05$.

Competing interests

The authors declare no competing interests.

Received: 2 July 2024 / Accepted: 5 November 2024

Published online: 23 November 2024

References

- Adams TS, et al. Single-cell RNA-seq reveals ectopic and aberrant lung-resident cell populations in idiopathic pulmonary fibrosis. *Sci Adv.* 2020;6:eaba1983.
- Alsafadi HN, et al. An ex vivo model to induce early fibrosis-like changes in human precision-cut lung slices. *Am J Physiol Lung Cell Mol Physiol.* 2017;312:L896–902.
- Alysandratos KD, et al. Culture impact on the transcriptomic programs of primary and iPSC-derived human alveolar type 2 cells. *JCI Insight.* 2022.
- Aros CJ, Pantoja CJ, Gomperts BN. Wnt signaling in lung development, regeneration, and disease progression. *Commun Biol.* 2021;4:601.
- Barkauskas CE, et al. Type 2 alveolar cells are stem cells in adult lung. *J Clin Invest.* 2013;123:3025–36.
- Barnes PJ, Baker J, Donnelly LE. Cellular Senescence as a mechanism and target in Chronic Lung diseases. *Am J Respir Crit Care Med.* 2019;200:556–64.
- Borie R, et al. The MUC5B variant is associated with idiopathic pulmonary fibrosis but not with systemic sclerosis interstitial lung disease in the European caucasian population. *PLoS ONE.* 2013;8:e70621.
- Borie R, et al. Colocalization of Gene expression and DNA methylation with genetic risk variants supports functional roles of MUC5B and DSP in Idiopathic Pulmonary Fibrosis. *Am J Respir Crit Care Med.* 2022;206:1259–70.
- Brand M, et al. Biochemical and transcriptomic evaluation of a 3D lung organoid platform for pre-clinical testing of active substances targeting senescence. *Respir Res.* 2024;25:3.
- Chaib S, Tchkonja T, Kirkland JL. Cellular senescence and senolytics: the path to the clinic. *Nat Med.* 2022;28:1556–68.
- Conti C, et al. Mucins MUC5B and MUC5AC in Distal Airways and Honeycomb spaces: comparison among idiopathic pulmonary Fibrosis/Usual interstitial pneumonia, Fibrotic nonspecific interstitial pneumonitis, and control lungs. *Am J Respir Crit Care Med.* 2016;193:462–4.
- Fingerlin TE, et al. Genome-wide association study identifies multiple susceptibility loci for pulmonary fibrosis. *Nat Genet.* 2013;45:613–20.
- Ghonim MA, Boyd DF, Flerlage T, Thomas PG. (2023) Pulmonary inflammation and fibroblast immunoregulation: from bench to bedside. *J Clin Invest* 133.
- Guarnier LP et al. (2023) Regenerative and translational medicine in COPD: hype and hope. *Eur Respir Rev* 32.
- Guo L, Chen Q, Xu M, Huang J, Ye H. Communication between alveolar macrophages and fibroblasts via the TNFSF12-TNFRSF12A pathway promotes pulmonary fibrosis in severe COVID-19 patients. *J Transl Med.* 2024;22:698.
- Habermann AC, et al. Single-cell RNA sequencing reveals profibrotic roles of distinct epithelial and mesenchymal lineages in pulmonary fibrosis. *Sci Adv.* 2020;6:eaba1972.
- Hamsanathan S, et al. Cellular Senescence: the Trojan Horse in Chronic Lung diseases. *Am J Respir Cell Mol Biol.* 2019;61:21–30.
- Hancock LA, et al. Muc5b overexpression causes mucociliary dysfunction and enhances lung fibrosis in mice. *Nat Commun.* 2018;9:5363.
- Herrera JA et al. (2022) The UIP/IPF fibroblastic focus is a collagen biosynthesis factory embedded in a distinct extracellular matrix. *JCI Insight* 7.
- Jacob A, et al. Differentiation of human pluripotent stem cells into functional lung alveolar epithelial cells. *Cell Stem Cell.* 2017;21:472–e488410.
- Jaeger B, et al. Airway basal cells show a dedifferentiated KRT17(high)phenotype and promote fibrosis in idiopathic pulmonary fibrosis. *Nat Commun.* 2022;13:5637.
- Jia M, et al. Early events marking lung fibroblast transition to profibrotic state in idiopathic pulmonary fibrosis. *Respir Res.* 2023;24:116.
- Juul NH, Stockman CA, Desai TJ. (2020) Niche Cells and Signals that regulate lung alveolar stem cells in vivo. *Cold Spring Harb Perspect Biol* 12.
- Kastlmeier MT, et al. Cytokine signaling converging on IL11 in ILD fibroblasts provokes aberrant epithelial differentiation signatures. *Front Immunol.* 2023;14:1128239.
- Kathiriyi JJ, et al. Human alveolar type 2 epithelium transdifferentiates into meta-plastic KRT5(+) basal cells. *Nat Cell Biol.* 2022;24:10–23.
- Katsura H, et al. Human lung stem cell-based alveolospheres provide insights into SARS-CoV-2-Mediated Interferon responses and pneumocyte dysfunction. *Cell Stem Cell.* 2020;27:890–904. e898.
- Kohli J, et al. Algorithmic assessment of cellular senescence in experimental and clinical specimens. *Nat Protoc.* 2021;16:2471–98.
- Konigshoff M, et al. WNT1-inducible signaling protein-1 mediates pulmonary fibrosis in mice and is upregulated in humans with idiopathic pulmonary fibrosis. *J Clin Invest.* 2009;119:772–87.
- Kurche JS, et al. Muc5b enhances murine honeycomb-like cyst formation. *Am J Respir Cell Mol Biol.* 2019;61:544–6.
- Le TT, et al. Blockade of IL-6 trans signaling attenuates pulmonary fibrosis. *J Immunol.* 2014;193:3755–68.
- Lee JH, et al. Anatomically and functionally distinct lung mesenchymal populations marked by Lgr5 and Lgr6. *Cell.* 2017;170:1149–e11631112.
- Lehmann M, et al. Differential effects of Nintedanib and Pirfenidone on lung alveolar epithelial cell function in ex vivo murine and human lung tissue cultures of pulmonary fibrosis. *Respir Res.* 2018;19:175.
- Liang J, et al. Hyaluronan and TLR4 promote surfactant-protein-C-positive alveolar progenitor cell renewal and prevent severe pulmonary fibrosis in mice. *Nat Med.* 2016;22:1285–93.
- Martinez FJ, et al. Idiopathic pulmonary fibrosis. *Nat Rev Dis Primers.* 2017;3:17074.
- Melo-Narvaez MC et al. (2024) Stimuli-Specific Senescence of Primary Human Lung Fibroblasts Modulates Alveolar Stem Cell Function. *Cells* 13.
- Michalski JE, Schwartz DA. Genetic risk factors for idiopathic pulmonary fibrosis: insights into immunopathogenesis. *J Inflamm Res.* 2020;13:1305–18.
- Milad N, Morissette MC. (2021) Revisiting the role of pulmonary surfactant in chronic inflammatory lung diseases and environmental exposure. *Eur Respir Rev* 30.
- Moiseeva V, et al. Senescence Atlas reveals an aged-like inflamed niche that blunts muscle regeneration. *Nature.* 2023;613:169–78.
- Moore C, et al. Resequencing Study confirms that host defense and cell senescence gene variants contribute to the risk of idiopathic pulmonary fibrosis. *Am J Respir Crit Care Med.* 2019;200:199–208.
- Murthy KL P, et al. Human distal lung maps and lineage hierarchies reveal a bipotent progenitor. *Nature.* 2022;604:111–9.
- Nguyen HN, et al. Autocrine Loop Involving IL-6 family member LIF, LIF receptor, and STAT4 drives sustained fibroblast production of Inflammatory mediators. *Immunity.* 2017;46:220–32.
- O'Donoghue RJ, et al. Genetic partitioning of interleukin-6 signalling in mice dissociates Stat3 from Smad3-mediated lung fibrosis. *EMBO Mol Med.* 2012;4:939–51.
- Parimon T, Yao C, Stripp BR, Noble PW, Chen P. (2020) Alveolar epithelial type II cells as drivers of lung fibrosis in idiopathic pulmonary fibrosis. *Int J Mol Sci* 21.
- Paris AJ, et al. STAT3-BDNF-TrkB signalling promotes alveolar epithelial regeneration after lung injury. *Nat Cell Biol.* 2020;22:1197–210.

- Pedroza M, et al. STAT-3 contributes to pulmonary fibrosis through epithelial injury and fibroblast-myofibroblast differentiation. *FASEB J*. 2016;30:129–40.
- Peljto AL, et al. The MUC5B promoter polymorphism is associated with idiopathic pulmonary fibrosis in a Mexican cohort but is rare among Asian ancestries. *Chest*. 2015;147:460–4.
- Peysers R, et al. Defining the activated Fibroblast Population in Lung Fibrosis using single-cell sequencing. *Am J Respir Cell Mol Biol*. 2019;61:74–85.
- Ptasinski V et al. (2023) Modeling fibrotic alveolar transitional cells with pluripotent stem cell-derived alveolar organoids. *Life Sci Alliance* 6.
- Qiu X, et al. Reversed graph embedding resolves complex single-cell trajectories. *Nat Methods*. 2017;14:979–82.
- Riccetti M, Gokey JJ, Aronow B, Perl AT. The elephant in the lung: integrating lineage-tracing, molecular markers, and single cell sequencing data to identify distinct fibroblast populations during lung development and regeneration. *Matrix Biol*. 2020;91–92:51–74.
- Saul D, et al. A new gene set identifies senescent cells and predicts senescence-associated pathways across tissues. *Nat Commun*. 2022;13:4827.
- Seibold MA, et al. A common MUC5B promoter polymorphism and pulmonary fibrosis. *N Engl J Med*. 2011;364:1503–12.
- Sikkema L, et al. An integrated cell atlas of the lung in health and disease. *Nat Med*. 2023;29:1563–77.
- Sprott RF, et al. Flagellin shifts 3D bronchospheres towards mucus hyperproduction. *Respir Res*. 2020;21:222.
- Stock CJ, et al. Mucin 5B promoter polymorphism is associated with idiopathic pulmonary fibrosis but not with development of lung fibrosis in systemic sclerosis or sarcoidosis. *Thorax*. 2013;68:436–41.
- Tsukui T, et al. Collagen-producing lung cell atlas identifies multiple subsets with distinct localization and relevance to fibrosis. *Nat Commun*. 2020;11:1920.
- Tsukui T, Wolters PJ, Sheppard D. Alveolar fibroblast lineage orchestrates lung inflammation and fibrosis. *Nature*. 2024;631:627–34.
- Ushakumary MG, Riccetti M, Perl AT. Resident interstitial lung fibroblasts and their role in alveolar stem cell niche development, homeostasis, injury, and regeneration. *Stem Cells Transl Med*. 2021;10:1021–32.
- Woldhuis RR, et al. COPD-derived fibroblasts secrete higher levels of senescence-associated secretory phenotype proteins. *Thorax*. 2021;76:508–11.
- Yao Y et al. (2023) Mutual regulation of transcriptomes between murine pneumocytes and fibroblasts mediates alveolar regeneration in Air-Liquid interface cultures. *Am J Respir Cell Mol Biol*.
- Yao Y, et al. Mutual regulation of transcriptomes between murine pneumocytes and fibroblasts mediates alveolar regeneration in Air-Liquid interface cultures. *Am J Respir Cell Mol Biol*. 2024;70:203–14.
- Ye Z, Hu Y. (2021) TGF- β 1: gentlemanly orchestrator in idiopathic pulmonary fibrosis (review). *Int J Mol Med* 48.
- Zacharias WJ, et al. Regeneration of the lung alveolus by an evolutionarily conserved epithelial progenitor. *Nature*. 2018;555:251–5.
- Zepp JA, et al. Distinct mesenchymal lineages and niches promote epithelial Self-Renewal and Myofibrogenesis in the lung. *Cell*. 2017;170:1134–e11481110.
- Zhang Y, Noth I, Garcia JG, Kaminski N. A variant in the promoter of MUC5B and idiopathic pulmonary fibrosis. *N Engl J Med*. 2011;364:1576–7.
- Zhu Y, et al. The Achilles' heel of senescent cells: from transcriptome to senolytic drugs. *Aging Cell*. 2015;14:644–58.

Publisher's note

Springer Nature remains neutral with regard to jurisdictional claims in published maps and institutional affiliations.